Y3.N21/5:6/1741
GOVT. DOC.

NACA TN No. 1741

NATIONAL ADVISORY COMMITTEE FOR AERONAUTICS

TECHNICAL NOTE

No. 1741

EXPLORATORY WIND-TUNNEL INVESTIGATION OF THE EFFECTIVENESS OF AREA SUCTION IN ELIMINATING LEADING-EDGE SEPARATION OVER AN NACA 64_1A212 AIRFOIL

By Robert J. Nuber and James R. Needham, Jr.

Langley Aeronautical Laboratory
Langley Field, Va.

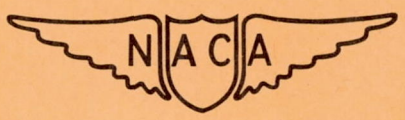

Washington

November 1948

CONN. STATE LIBRARY

NOV 26 1948

BUSINESS, SCIENCE & TECHNOLOGY DEP'T.

NATIONAL ADVISORY COMMITTEE FOR AERONAUTICS

TECHNICAL NOTE NO. 1741

EXPLORATORY WIND-TUNNEL INVESTIGATION OF THE EFFECTIVENESS OF AREA SUCTION IN ELIMINATING LEADING-EDGE SEPARATION OVER AN NACA 64_1A212 AIRFOIL

By Robert J. Nuber and James R. Needham, Jr.

SUMMARY

An exploratory investigation was made in the Langley two-dimensional low-turbulence pressure tunnel on an NACA 64_1A212 airfoil with various extents of permeable surface area between the leading edge and 12.5 percent chord to determine the effectiveness of area suction in eliminating leading-edge separation at high lift coefficients. Lift and internal pressure measurements were obtained at a Reynolds number of 1.5×10^6 for a range of flow coefficients from 0 to 0.008. Airfoil surface pressures were measured over a range of angles of attack from 4.1° to 18.3° with the upper surface porous to 4.5 percent chord.

The results obtained indicate that not only was leading-edge separation prevented, but also turbulent separation moving forward from the trailing edge was delayed. The maximum effectiveness was obtained at a flow coefficient of 0.0018 with the upper surface porous to 4.5 percent chord. With more than 4.5 percent chord permeable, the maximum section lift coefficient $c_{l_{max}}$ of the airfoil was not changed appreciably, but the flow coefficient required to obtain $c_{l_{max}}$ was considerably increased. It was also determined that for this airfoil at a similar Reynolds number the maximum section lift coefficient is about the same as that for the airfoil with a leading-edge slat.

INTRODUCTION

The maximum lift coefficients of thin airfoil sections are low as a result of separation of the laminar boundary layer near the leading edge. Many types of leading-edge high-lift devices, such as flaps and slats, have been investigated in an attempt to increase these naturally low maximum lift coefficients. Single suction slots near the leading edge also have been investigated but proved unsatisfactory because of changes in the position of the laminar separation point with variations in angle

of attack. Area suction through a permeable surface near the leading edge appeared to offer a method of applying boundary-layer suction to control laminar separation. An exploratory investigation has been made accordingly in the Langley two-dimensional low-turbulence pressure tunnel to determine the effectiveness of area suction through a permeable surface at the leading edge in controlling leading-edge separation.

An NACA 64_1A212 airfoil section was employed in the present investigation because the results presented in reference 1 show the maximum lift of this airfoil to be limited by separation of the laminar boundary layer near the leading edge. The effect of variations of the relative extent of permeable surface area was investigated. The tests included measurements at a Reynolds number of 1.5×10^6 of lift, internal pressure, and airfoil surface pressures over a range of flow coefficients from 0 to 0.008.

SYMBOLS

c_l	section lift coefficient $\left(\frac{l}{q_o c}\right)$
$c_{l_{max}}$	maximum section lift coefficient
c	airfoil chord (24 in.)
l	airfoil lift per unit span
b	span of porous surface (34.45 in.)
V_o	free-stream velocity
ρ_o	free-stream mass density
q_o	free-stream dynamic pressure $\left(\frac{1}{2}\rho_o V_o^2\right)$
Q	volume of air removed through porous surface per unit time
C_Q	flow coefficient $\left(\frac{Q}{cbV_o}\right)$
H_o	free-stream total pressure
H_b	total pressure inside wing duct
C_P	internal pressure coefficient $\left(\frac{H_o - H_b}{q_o}\right)$
α_o	section angle of attack, degrees
p	local static pressure

S	airfoil pressure coefficient $\left(\frac{H_o - p}{q_o}\right)$
S_{max}	airfoil peak pressure coefficient
R	Reynolds number $\left(\frac{V_o c}{\nu}\right)$
ν	kinematic viscosity
x	horizontal distance behind leading edge
y	vertical distance from chord line

MODEL

The 24-inch-chord cast aluminum model used in this investigation was constructed to the profile of an NACA 64_1A212 airfoil. The leading edge was formed with a continuous sheet of porous bronze extending to 12.5 percent chord on both surfaces. Ordinates of the airfoil section and a sketch of the model showing the general arrangement of the leading edge and ducting system are presented in table I and figure 1, respectively.

The sintered bronze material used as the permeable surface consisted of spherical particles ranging in size from 200 to 400 mesh which were coalesced into a sheet $\frac{3}{32}$-inch thick under controlled conditions of time, temperature, and atmosphere. The porosity was such that with air at approximately standard density the application of a suction of about 0.12 pounds per square inch induced an average velocity of 1.0 foot per second through the surface. Over a range of pressure differences from 0 to 2.0 pounds per square inch, the rate of flow through the porous surface varied nearly linearly with pressure difference.

Pressure orifices were installed on the airfoil surfaces from the leading edge to 12 percent of the chord (fig. 2) and were located 11.25 inches from the midspan in a single chordwise row. The chordwise positions of the orifices are given in the table of figure 2.

A plain wooden NACA 64_1A212 airfoil was used for the zero-flow condition.

APPARATUS AND TESTS

The model was tested in the Langley two-dimensional low-turbulence pressure tunnel and completely spanned the 36-inch-wide test section. The quantity of air removed from the boundary layer was determined by

means of an orifice plate located in the suction duct and was regulated by varying the orifice diameter and the blower speed.

A total-pressure tube in the wing duct on the end opposite that at which the air was removed was used to determine the loss in pressure incurred in sucking the boundary-layer air through the permeable surface. The velocities in the duct were so low that the static and total pressures were substantially equal. The airfoil pressure distribution was obtained from pressure orifices up to the 12-percent-chord station and over the remainder of the airfoil from a static-pressure tube, which, at each station, was bent approximately to the airfoil contour and was mounted approximately $\frac{1}{8}$ inch from the surface.

Airfoil lift and duct total pressure were measured through a range of angles of attack at flow coefficients up to 0.008 for various relative extents of permeable surface area. The amount of suction area was varied by applying strips of tape 0.003-inch thick to the porous surface in a spanwise direction allowing a $\frac{1}{4}$-inch clearance on either side of the pressure orifices.

The lift coefficients were measured and corrected to free-air conditions by the methods described in reference 2. All tests were made at a Reynolds number of 1.5×10^6 and a Mach number of 0.11. Small irregularities existed in the profile of the model near the leading edge but they appeared to have no appreciable effect on the aerodynamic characteristics.

RESULTS AND DISCUSSION

Lift

The lift and internal-pressure characteristics obtained from tests of the model for several flow coefficients are presented in the figures listed in the following table which designates the nose configuration corresponding to various relative extents of permeable surface area:

Figure number	Nose configuration	Permeable surfaces from L.E. (percent chord)	
		Upper surface	Lower surface
3(a)	A	12.5	12.5
3(b)	B	12.5	2.75
3(c)	C	12.5	0
3(d)	D	6.6	0
3(e)	E	4.5	0
3(f)	F	4.1	0

The effect of area suction on the variation of maximum section lift coefficient with flow coefficient for the nose configurations investigated is summarized in figure 4.

It is seen in figures 3 and 4 that, in general, the maximum section lift coefficient increased with increasing flow coefficient. These increases in maximum section lift coefficient with flow coefficient were accompanied by small increases in the angle of attack for maximum lift. With nose configuration A, the maximum section lift coefficient of the airfoil was increased from a value of 1.27 with no flow to a value of 1.6 for a flow coefficient of 0.008. This represents an increase in maximum lift of about 25 percent above the no-flow condition which was determined from tests of a plain wooden NACA 64_1A212 airfoil. For the airfoil equipped with a leading-edge slat (reference 1), the maximum section lift coefficient, obtained at a similar Reynolds number, was approximately the same as the highest $c_{l_{max}}$ obtained in the present investigation, but the angle of attack for $c_{l_{max}}$ was considerably lower for the model with leading-edge area suction.

As the permeable area on the lower surface was covered with strips of tape (fig. 4, configurations B and C) the values of the highest maximum section lift coefficient obtained were approximately the same as for configuration A, but the flow coefficient required to obtain this $c_{l_{max}}$ was reduced about 42 percent and 47 percent, respectively. Similarly, application of tape to the upper surface of the airfoil nose (configurations D and E) showed only a slight change in the highest $c_{l_{max}}$ from the value of 1.6 obtained for configuration A, but reductions in

the flow coefficient of about 73 percent and 77 percent, respectively, were obtained as compared with configuration A. The reductions in the relative extents of permeable surface area (configurations A to E), therefore, resulted in progressive reductions in the flow coefficient required for the highest maximum lift. As the permeable area on the upper surface was covered to 4.1 percent chord (configuration F), no appreciable changes in the flow coefficient (fig. 4) are noticed as compared with configuration E; however, the maximum section lift coefficient was reduced to a value of about 1.55. In view of this result, further covering of the permeable surfaces was discontinued and configuration E was considered to be the optimum.

Airfoil Pressure Distributions

Leading-edge separation was eliminated as soon as suction was applied. When the maximum section lift coefficient was obtained it was brought about by turbulent separation moving forward from the trailing edge. This result is shown in figure 5 which presents the airfoil surface pressures as a function of chordwise position (configuration E) for several flow coefficients over a range of angles of attack from 4.1° to 18.3°. As the angle of attack is increased from 4.1° to 12.2°, the airfoil is unstalled over the range of flow coefficients investigated. The peak pressures near the leading edge, as expected, increase rapidly with angle of attack and also increase with flow coefficient. In an attempt to explain the increase in peak pressure coefficient with increasing flow coefficient for the angle-of-attack range from 4° to 12°, the corresponding experimental increments in lift coefficient (fig. 3(e)) were expressed in terms of increased circulation, and with the aid of the known transformation function for the airfoil the resultant increase in peak pressure coefficient was calculated. It was found, however, that the measured increases in peak pressure coefficient were larger than the calculated values. The reason for these discrepancies is not definitely known, but they may possibly be attributed to an effective local increase in curvature of the airfoil near the leading edge caused by the flow into the porous surface. Increasing the angle of attack to 14.2° results in further increases in the peak pressures near the leading edge, accompanied by turbulent separation from the trailing edge which progresses forward along the upper surface of the airfoil with additional increases in angle of attack. Despite the existence of turbulent separation, the flow over the nose of the airfoil remained unseparated beyond the angle of attack for maximum lift (fig. 5(g)) even for the lowest flow coefficient investigated ($C_Q = 0.0005$). This result corroborates the theoretical work done by the British concerning leading-edge porous suction which indicates that very small amounts of suction are required to prevent leading-edge separation.

The extent of the separated region for a constant angle of attack (fig. 5) is shown to decrease progressively with increasing flow coefficient in spite of the increases in the peak negative pressures in the

region of the leading edge. This result is due to the very favorable effect of leading-edge suction on the conditions of the turbulent boundary layer.

The variation of airfoil peak pressure coefficient S_{max} and internal pressure coefficient C_p with angle of attack for configuration E is presented in figure 6. As shown in figure 6, for flow coefficients of 0.0005 and 0.0010 the curves of S_{max} and C_p cross at angles of attack of 10.3° and 15.1°, respectively. Beyond these angles of attack, S_{max} is greater than C_p; this result indicates that the pressure difference is in the direction to cause a local region of outflow. Despite the existence of outflow at these flow coefficients, laminar separation was prevented. An increase in the flow coefficient to 0.0018, where a large positive pressure difference is maintained, increased the maximum section lift coefficient (fig. 3(e)) to a value of 1.6. The fact that the highest maximum section lift coefficient was obtained with a flow coefficient of 0.0018 is attributable, therefore, to the favorable effects of increased flow coefficient on the conditions contributing to the development of the turbulent boundary layer.

In view of the increase in $c_{l_{max}}$ obtained with boundary-layer control in conjunction with a leading-edge slat (reference 1), further increases in $c_{l_{max}}$, above that obtained in the present investigation, will result from also controlling the turbulent boundary layer. Different distributions of suction over the leading-edge, particularly for thinner airfoils, should also be investigated by means of surfaces of different degrees of porosity in order to determine the configuration which will require the smallest amount of flow for optimum $c_{l_{max}}$.

CONCLUDING REMARKS

Results of an exploratory wind-tunnel investigation of area suction in eliminating leading-edge separation over an NACA 64_1A212 airfoil have been presented. It was found that not only was leading-edge separation prevented, but also turbulent separation moving forward from the trailing edge was delayed. The maximum effectiveness was obtained at a flow coefficient of 0.0018 with the upper surface porous to 4.5 percent chord. With more than 4.5 percent chord permeable, the maximum section lift coefficient $c_{l_{max}}$ of the airfoil was not changed appreciably, but the flow coefficient required to obtain $c_{l_{max}}$ was considerably increased. It was also determined that for this airfoil at a similar Reynolds

number the maximum section lift coefficient is about the same as that for the airfoil with a leading-edge slat.

Langley Aeronautical Laboratory
National Advisory Committee for Aeronautics
Langley Field, Va., August 18, 1948

REFERENCES

1. Quinn, John H., Jr.: Tests of the NACA 64_1A212 Airfoil Section with a Slat, a Double Slotted Flap and Boundary-Layer Control by Suction. NACA TN No. 1293, 1947.

2. Von Doenhoff, Albert E., and Abbott, Frank T., Jr.: The Langley Two-Dimensional Low-Turbulence Pressure Tunnel. NACA TN No. 1283, 1947.

TABLE I

NACA 64_1A212 AIRFOIL SECTION

[Stations and ordinates in percent airfoil chord]

Upper surface		Lower surface	
Station	Ordinate	Station	Ordinate
0	0	0	0
.409	1.013	.591	−.901
.648	1.233	.852	−1.075
1.135	1.580	1.365	−1.338
2.365	2.225	2.635	−1.803
4.849	3.145	5.151	−2.423
7.343	3.846	7.657	−2.874
9.842	4.432	10.158	−3.240
14.849	5.358	15.151	−3.796
19.862	6.060	20.138	−4.200
24.880	6.584	25.120	−4.482
29.900	6.956	30.100	−4.660
34.922	7.189	35.078	−4.741
39.946	7.272	40.054	−4.714
44.970	7.177	45.030	−4.549
49.993	6.935	50.007	−4.275
55.015	6.570	54.985	−3.918
60.034	6.103	59.966	−3.499
65.050	5.544	64.950	−3.034
70.064	4.903	69.936	−2.537
75.075	4.197	74.925	−2.037
80.090	3.433	79.910	−1.563
85.088	2.601	84.912	−1.159
90.062	1.751	89.938	−.771
95.032	.888	94.968	−.398
100.000	.025	99.999	−.025

L.E. radius: 0.994
Slope of radius through L.E.: 0.095

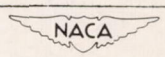

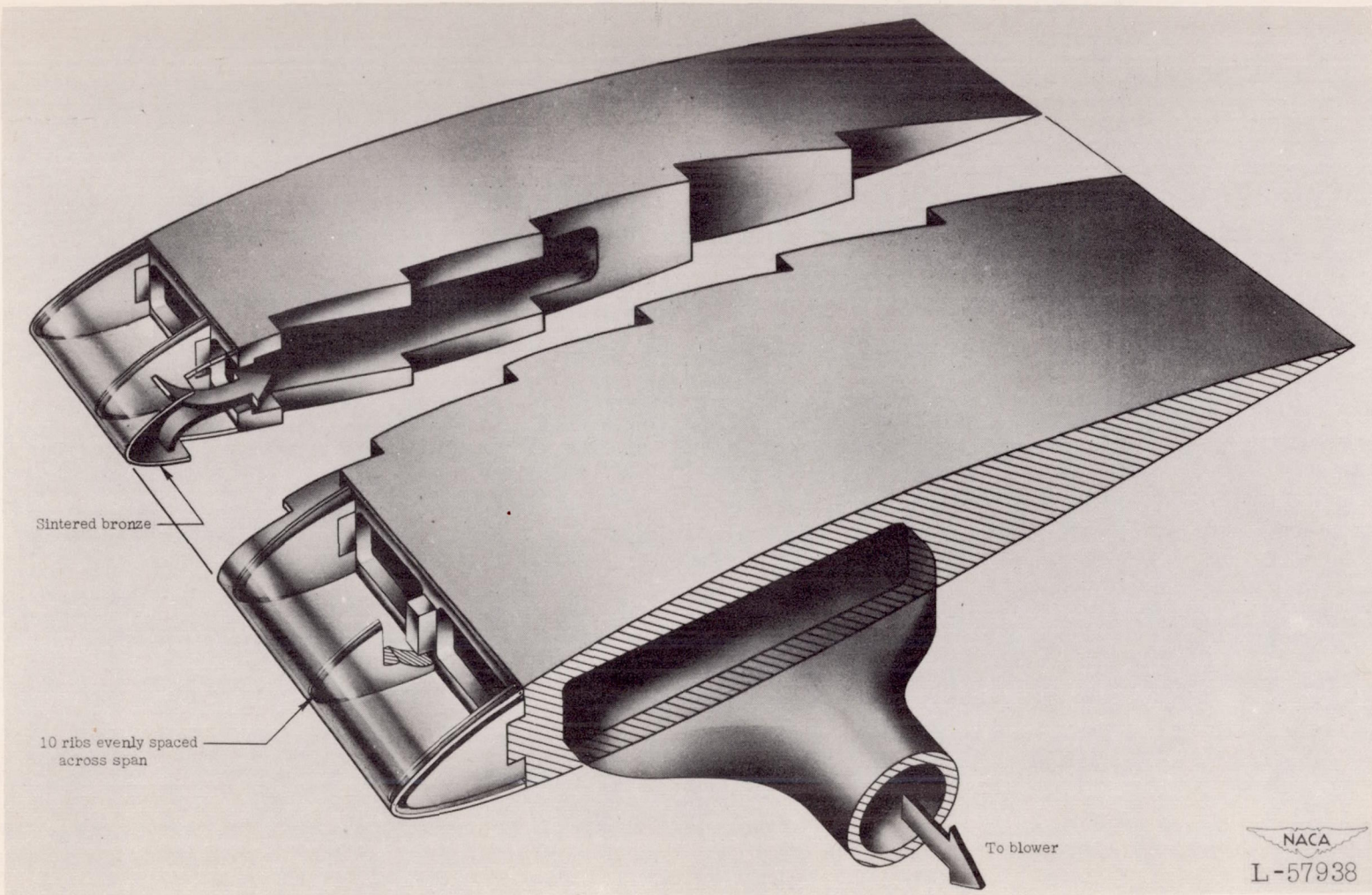

Figure 1.- Sketch of NACA 64_1A212 airfoil showing construction of leading edge and ducting system.

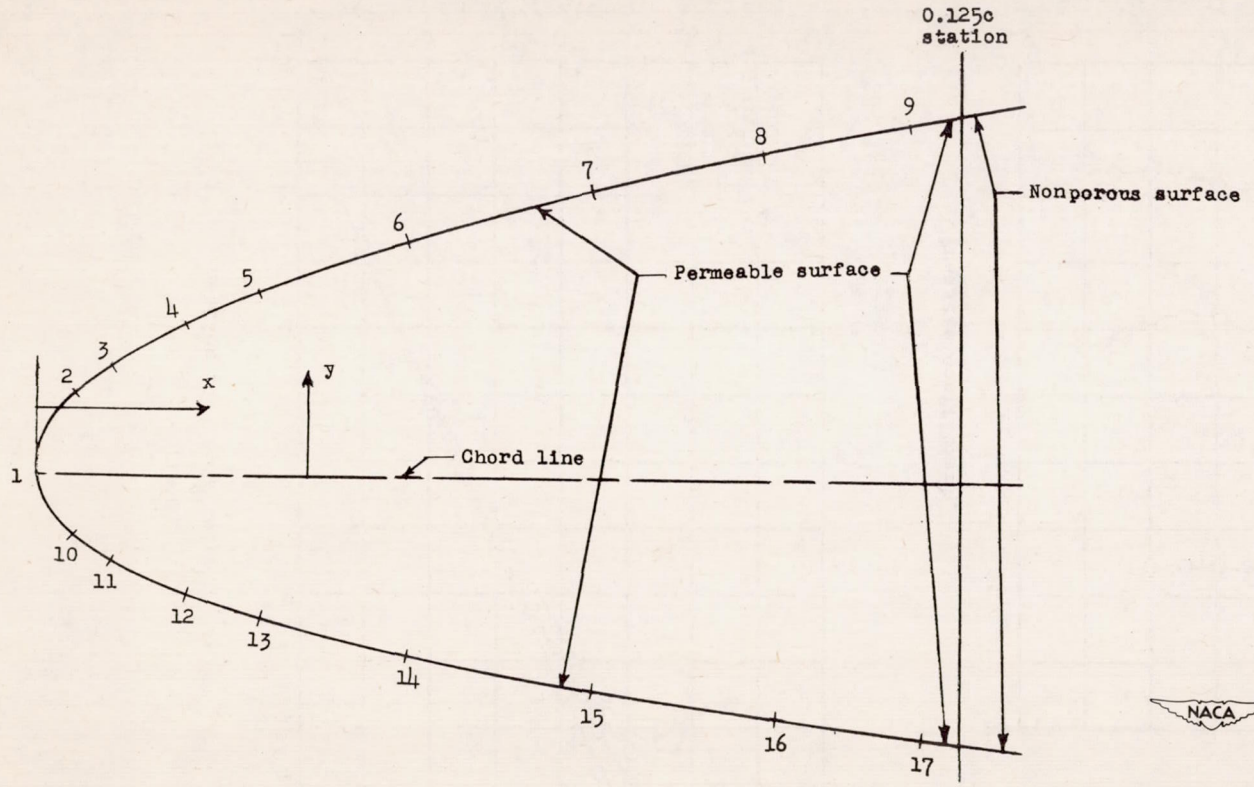

Orifice number	x/c	y/c
1	0	0
2	.5	1.104
3	1	1.492
4	2	2.054
5	3	2.492
6	5	3.183
7	7.5	3.888
8	9.8	4.429
9	11.8	4.817
10	.5	-.812
11	1	-1.146
12	2	-1.592
13	3	-1.904
14	5	-2.391
15	7.5	-2.862
16	10	-3.213
17	12	-3.468

Figure 2.- Location of pressure orifices on NACA 64_1A212 airfoil with permeable nose.

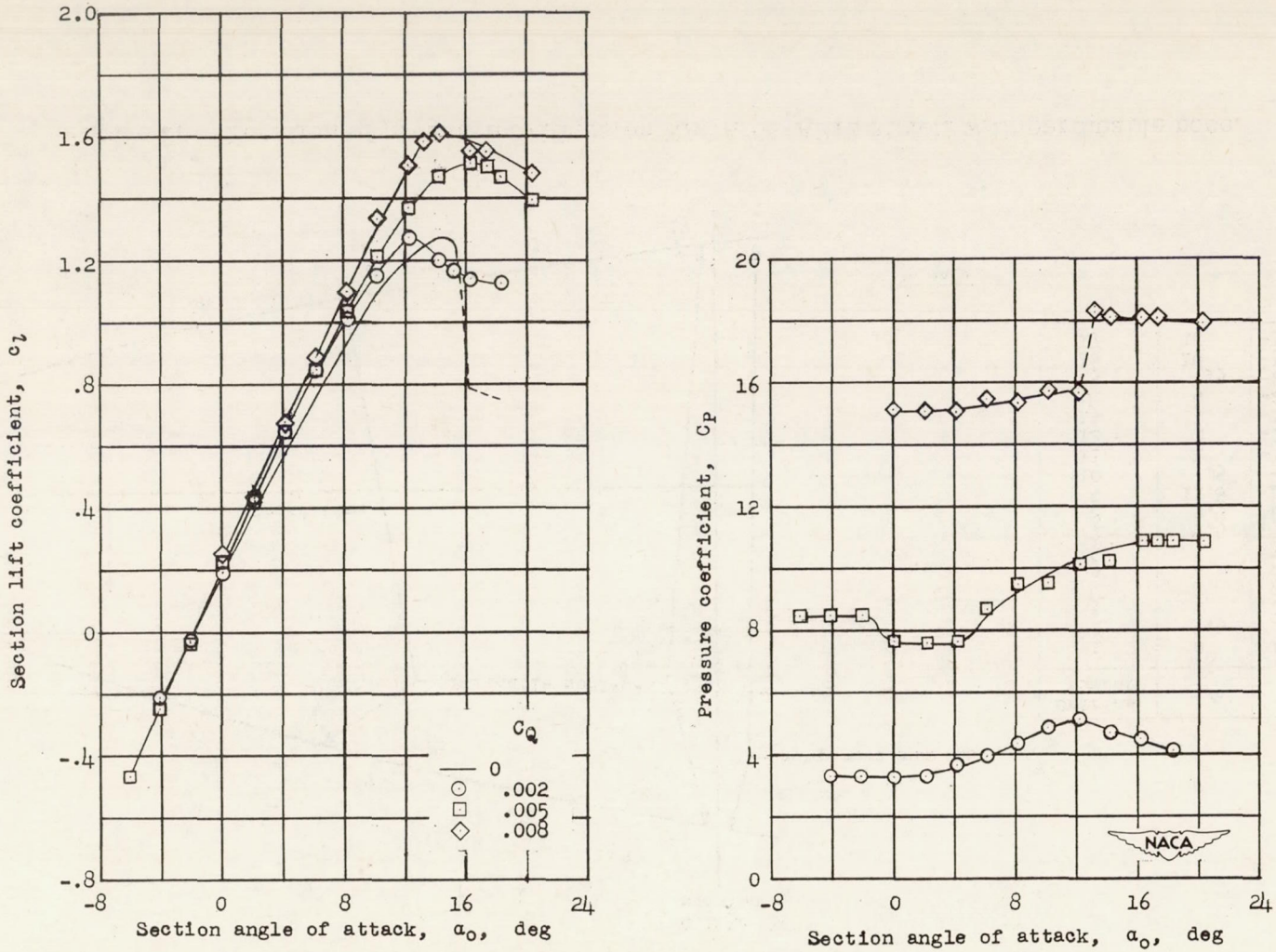

(a) Configuration A.

Figure 3.- Lift characteristics of an NACA 64_1A212 airfoil with permeable nose. $R \approx 1.5 \times 10^6$.

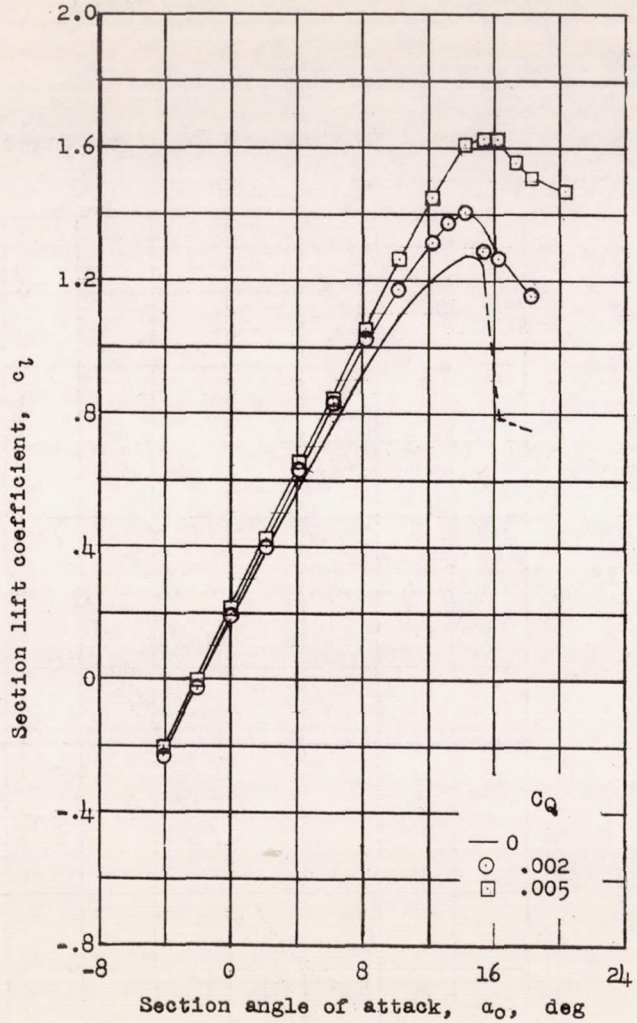

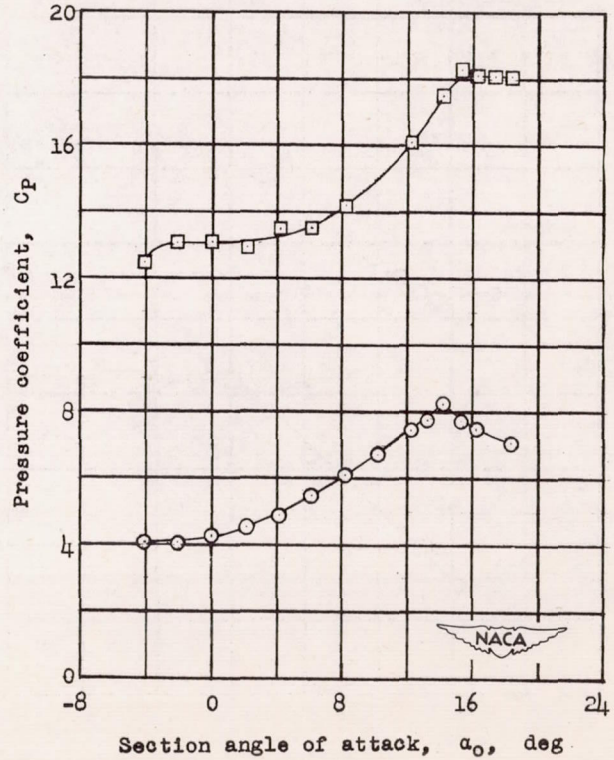

(b) Configuration B.

Figure 3.- Continued.

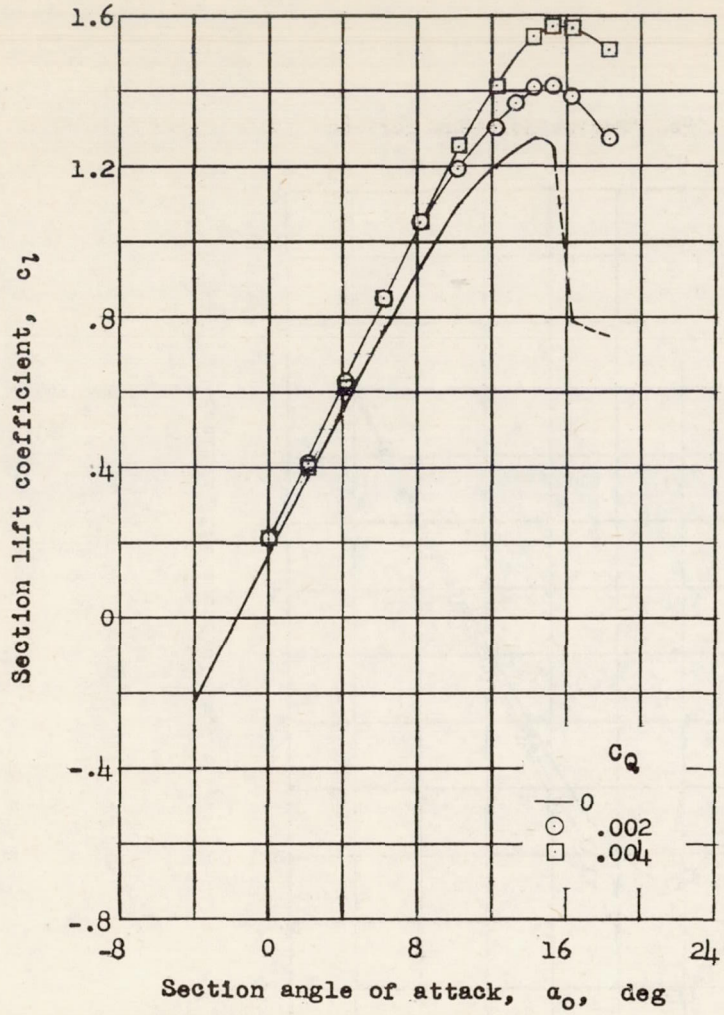

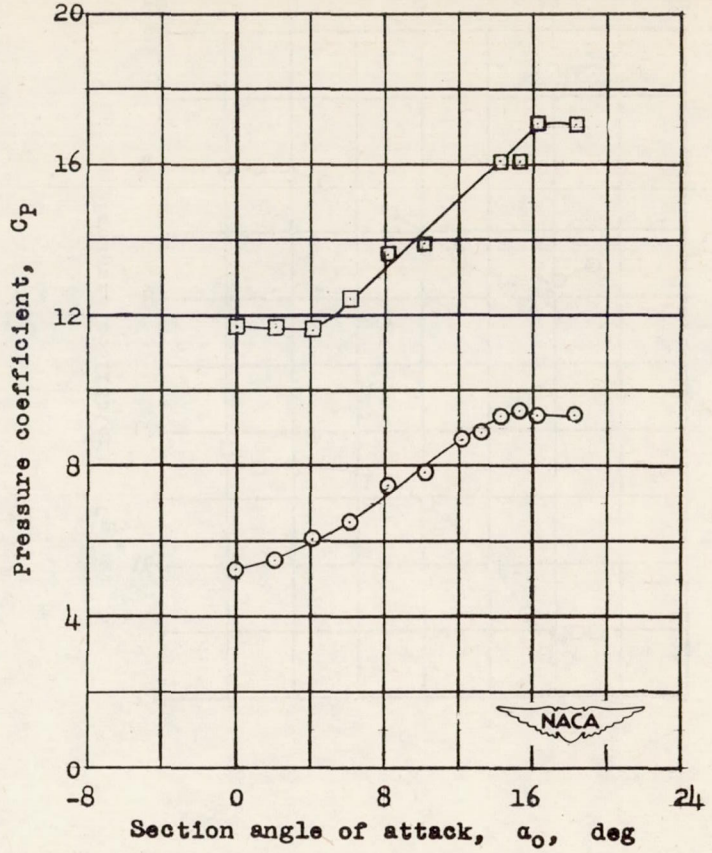

(c) Configuration C.

Figure 3.- Continued.

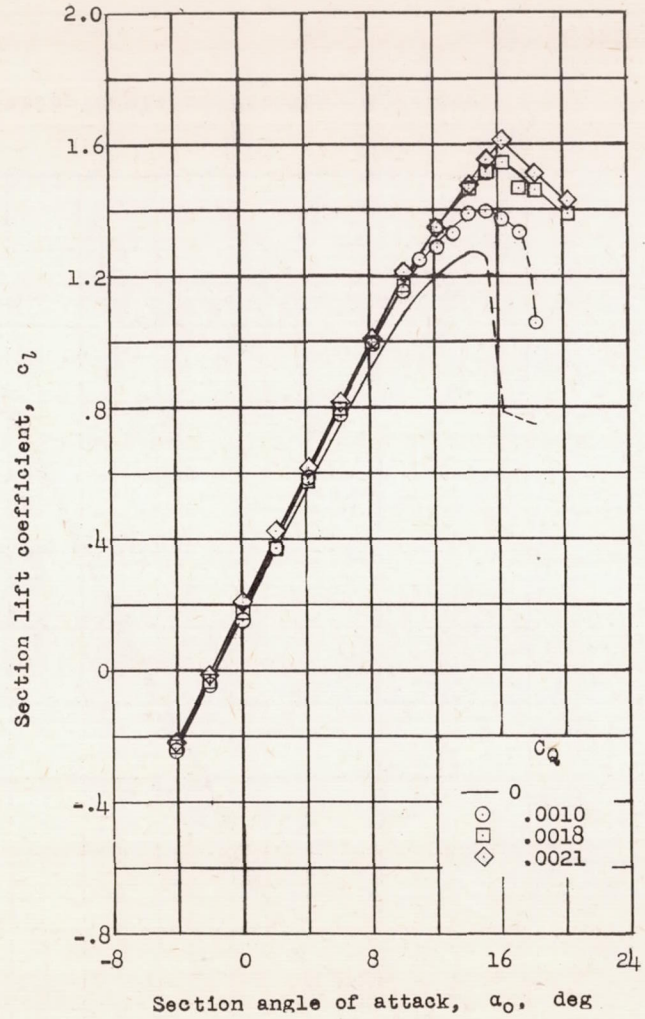

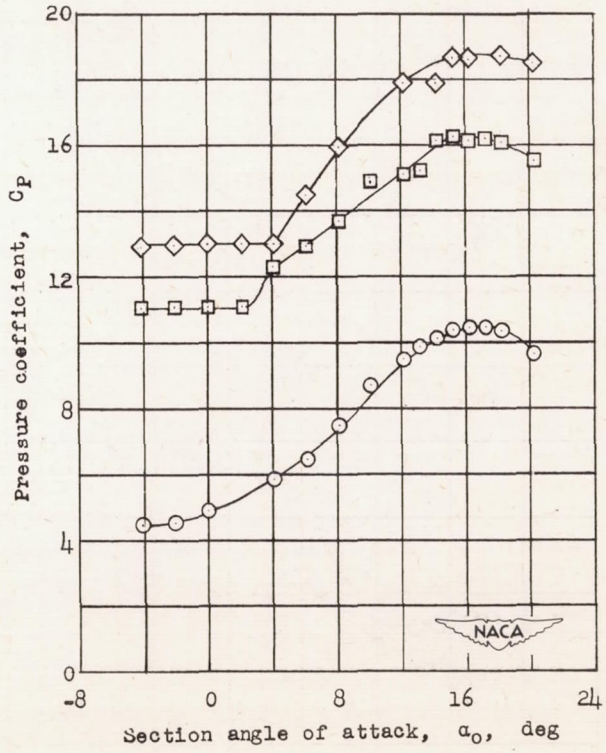

(d) Configuration D.

Figure 3.- Continued.

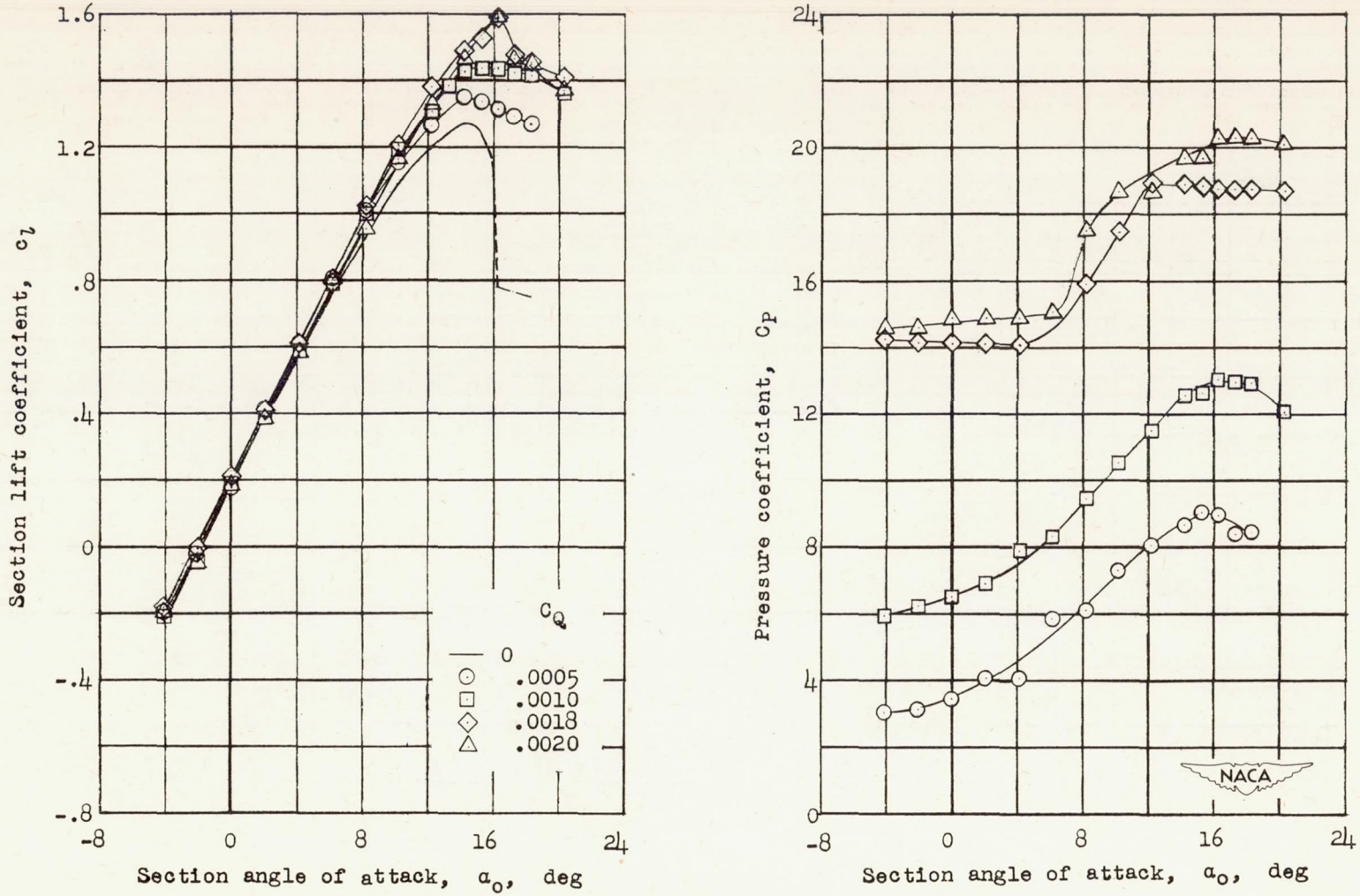

(e) Configuration E.

Figure 3.- Continued.

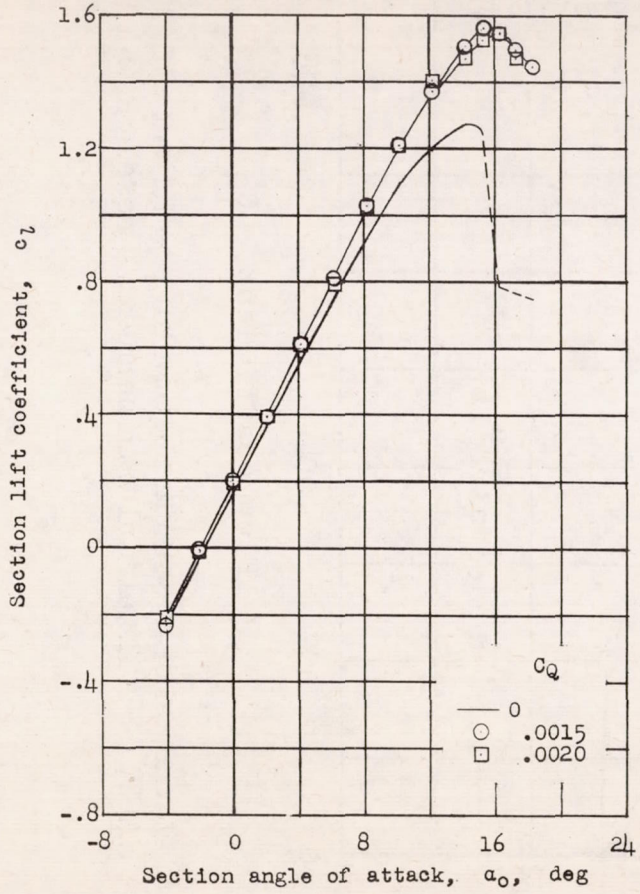

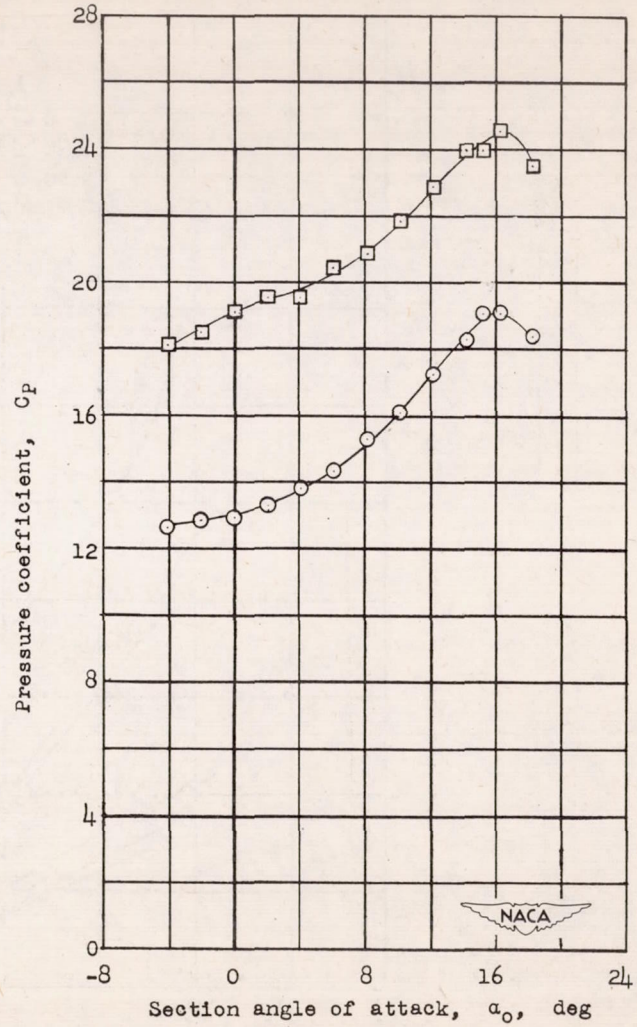

(f) Configuration F.

Figure 3.- Concluded.

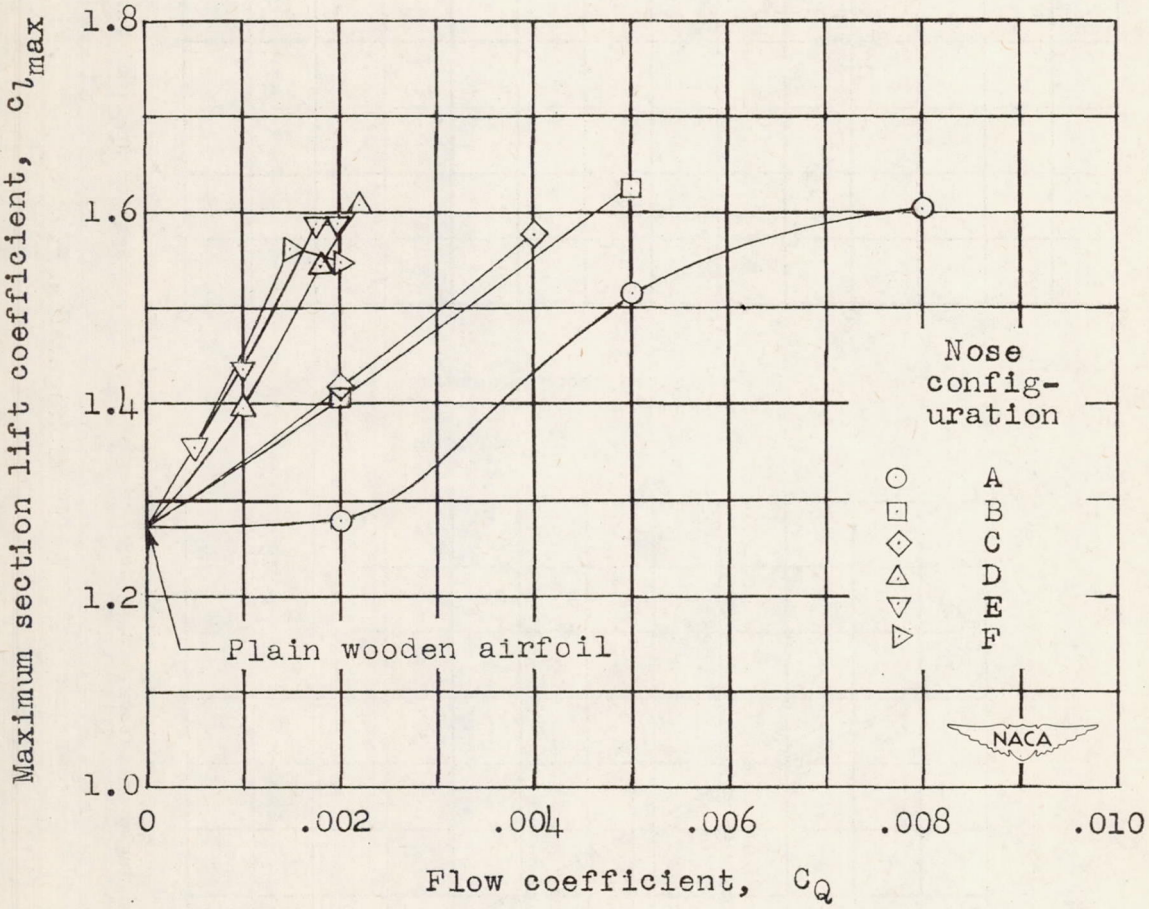

Figure 4.- Variation of maximum section lift coefficient with flow coefficient for the NACA 64_1A212 airfoil with permeable nose. $R \approx 1.5 \times 10^6$.

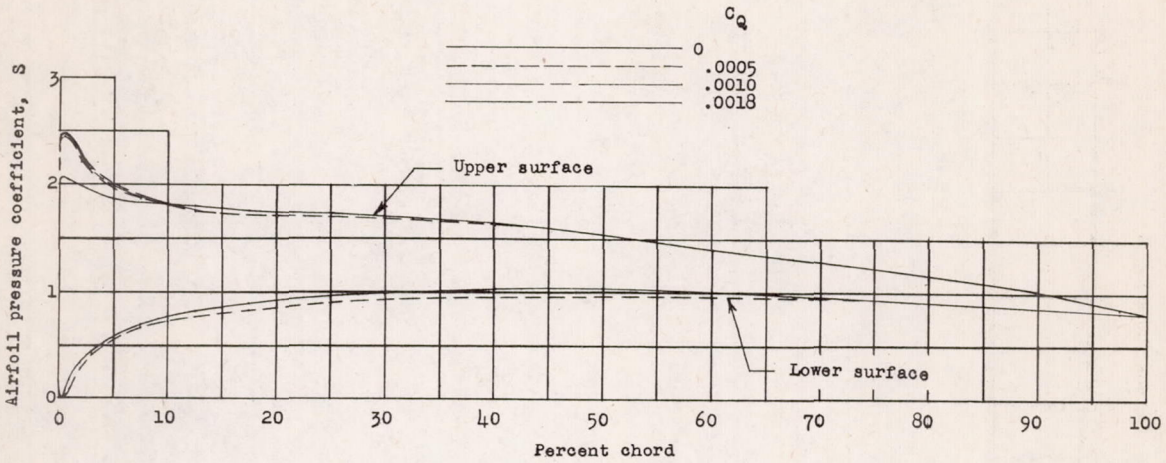

(a) $\alpha_o = 4.1^\circ$.

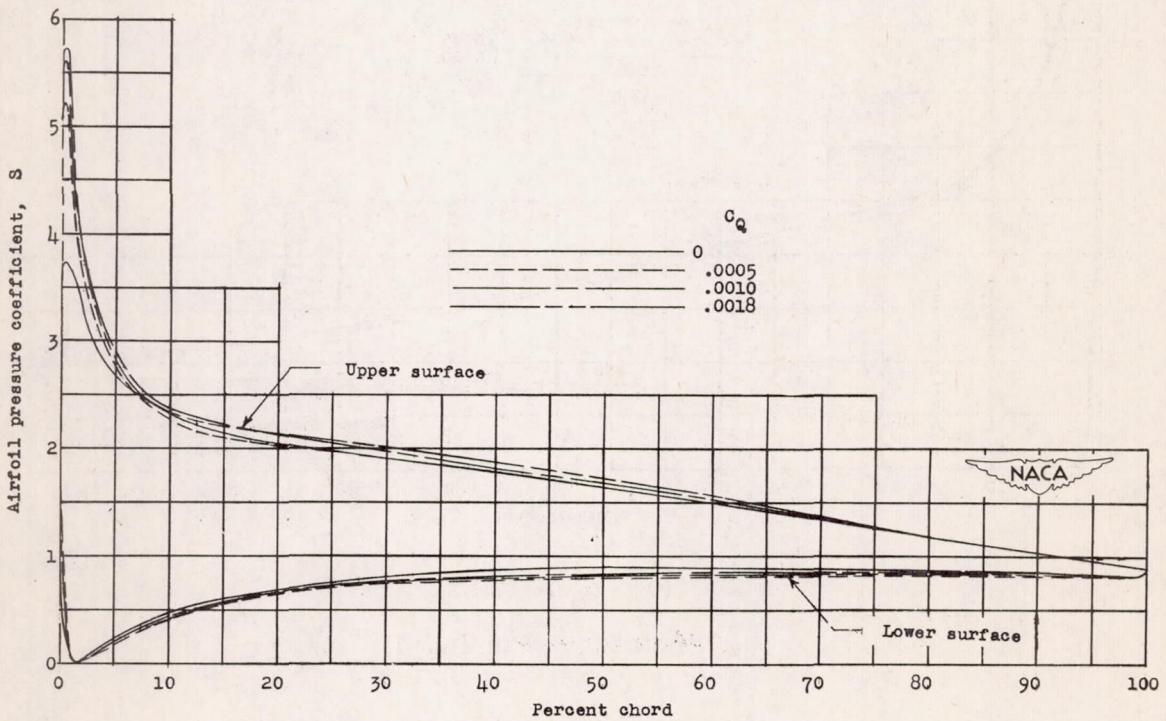

(b) $\alpha_o = 8.1^\circ$.

Figure 5.- Variation of pressure coefficient with percent chord for the NACA 64_1A212 airfoil with permeable nose. Configuration E; $R \approx 1.5 \times 10^6$.

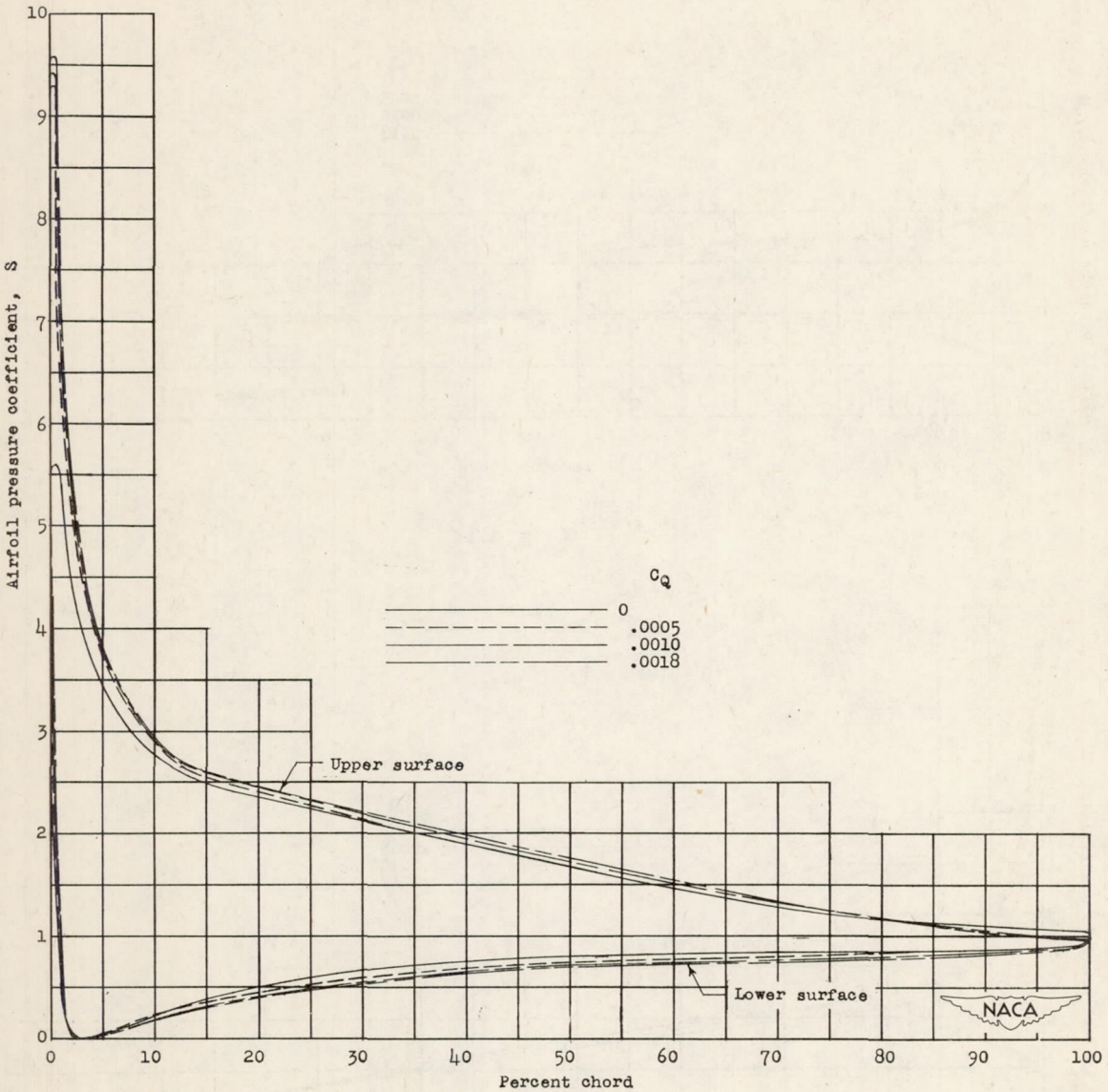

(c) $\alpha_o = 12.2^o$.

Figure 5.- Continued.

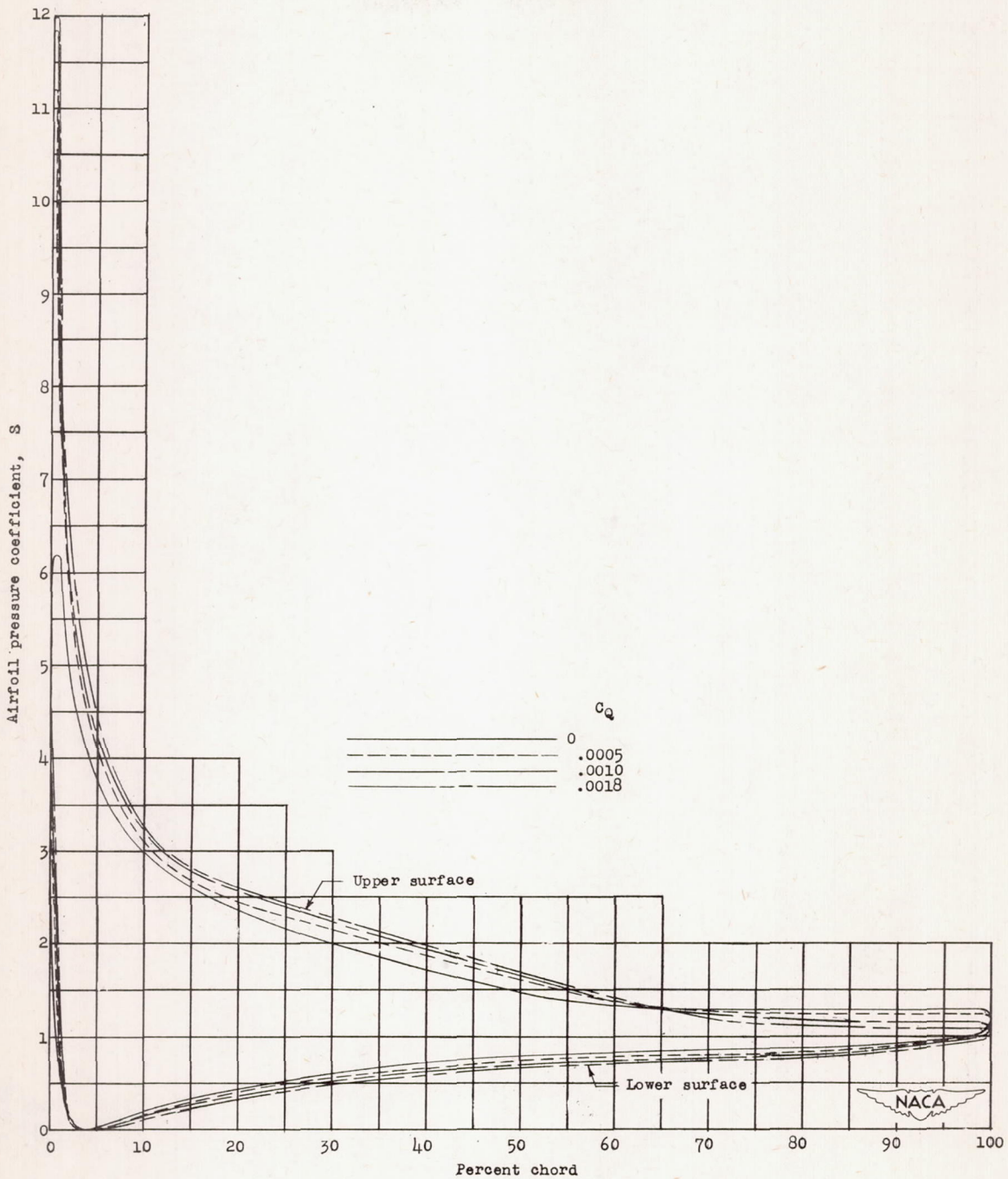

(d) $\alpha_o = 14.2^\circ$.

Figure 5.- Continued.

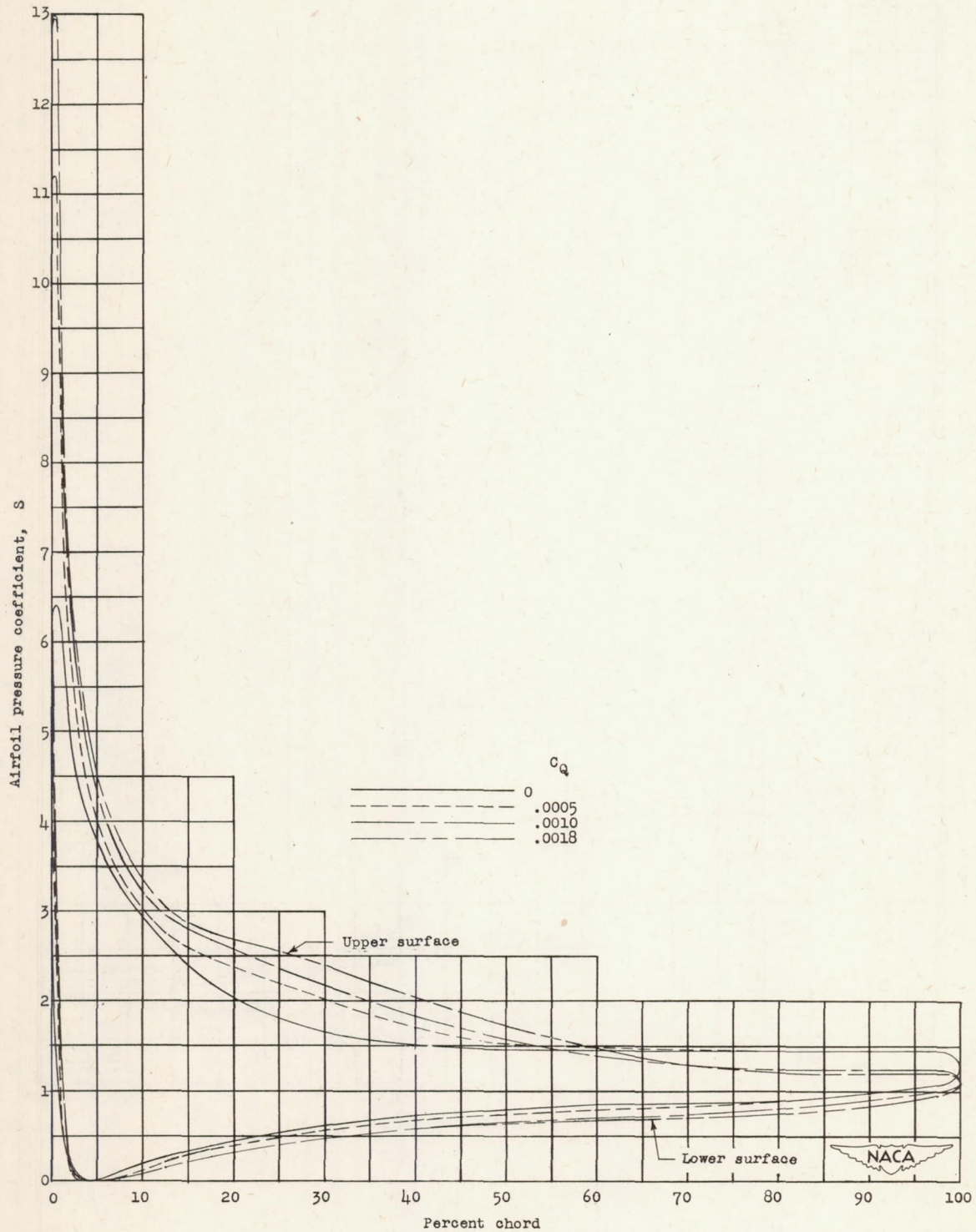

(e) $\alpha_o = 15.2^o$.

Figure 5.- Continued.

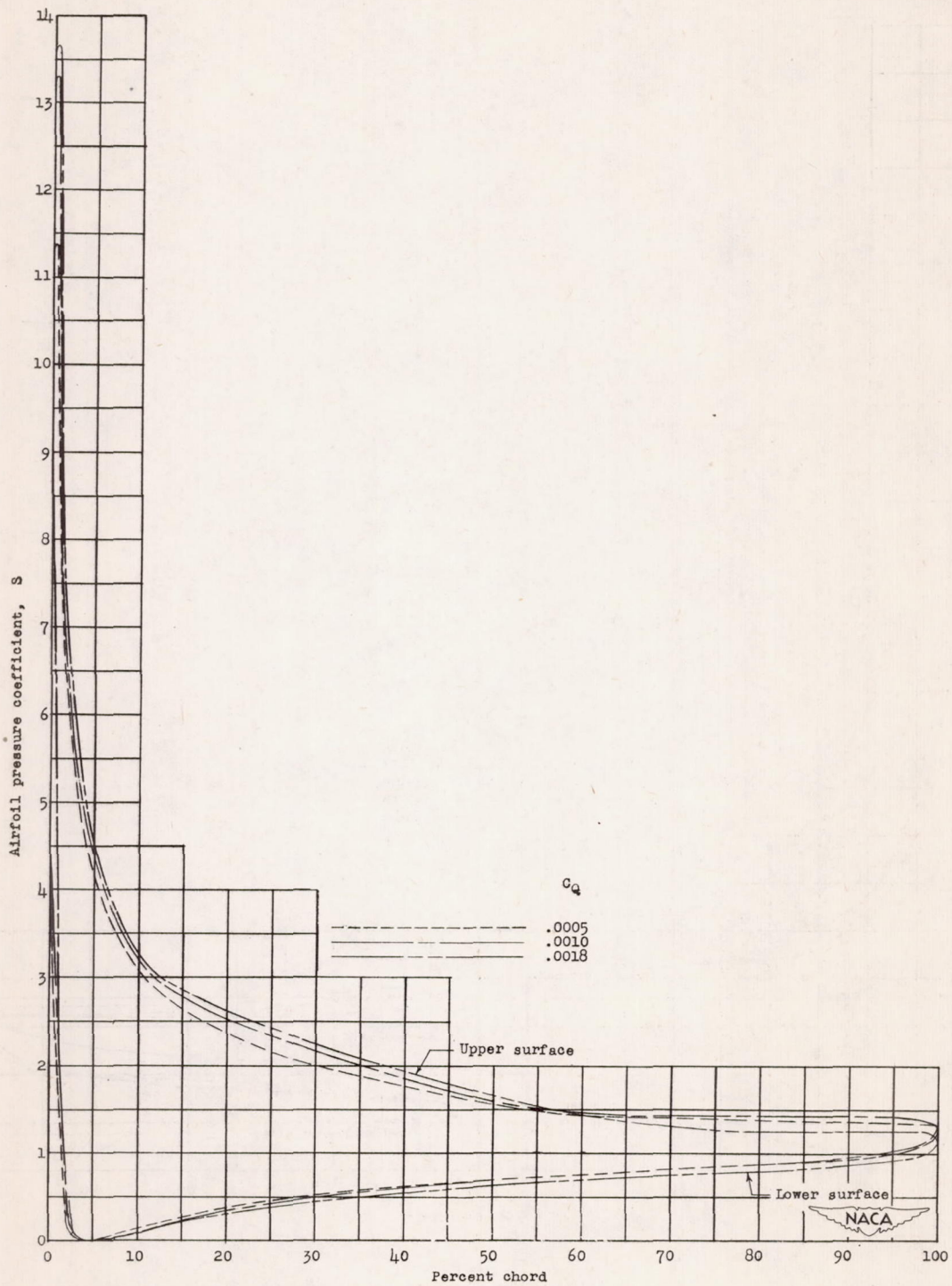

(f) $\alpha_o = 16.2^\circ$.

Figure 5.- Continued.

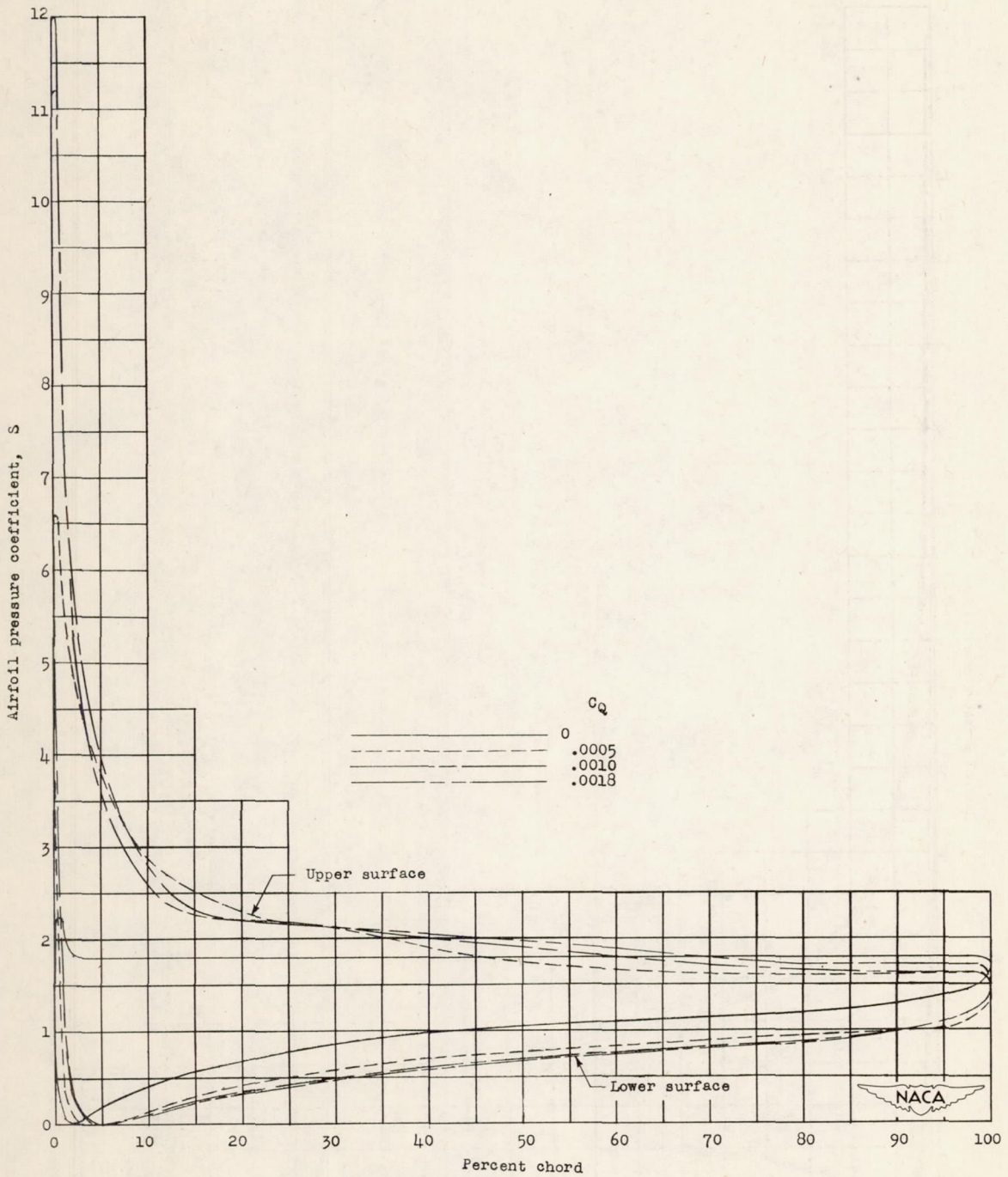

(g) $\alpha_o = 18.3^o$.

Figure 5.- Concluded.

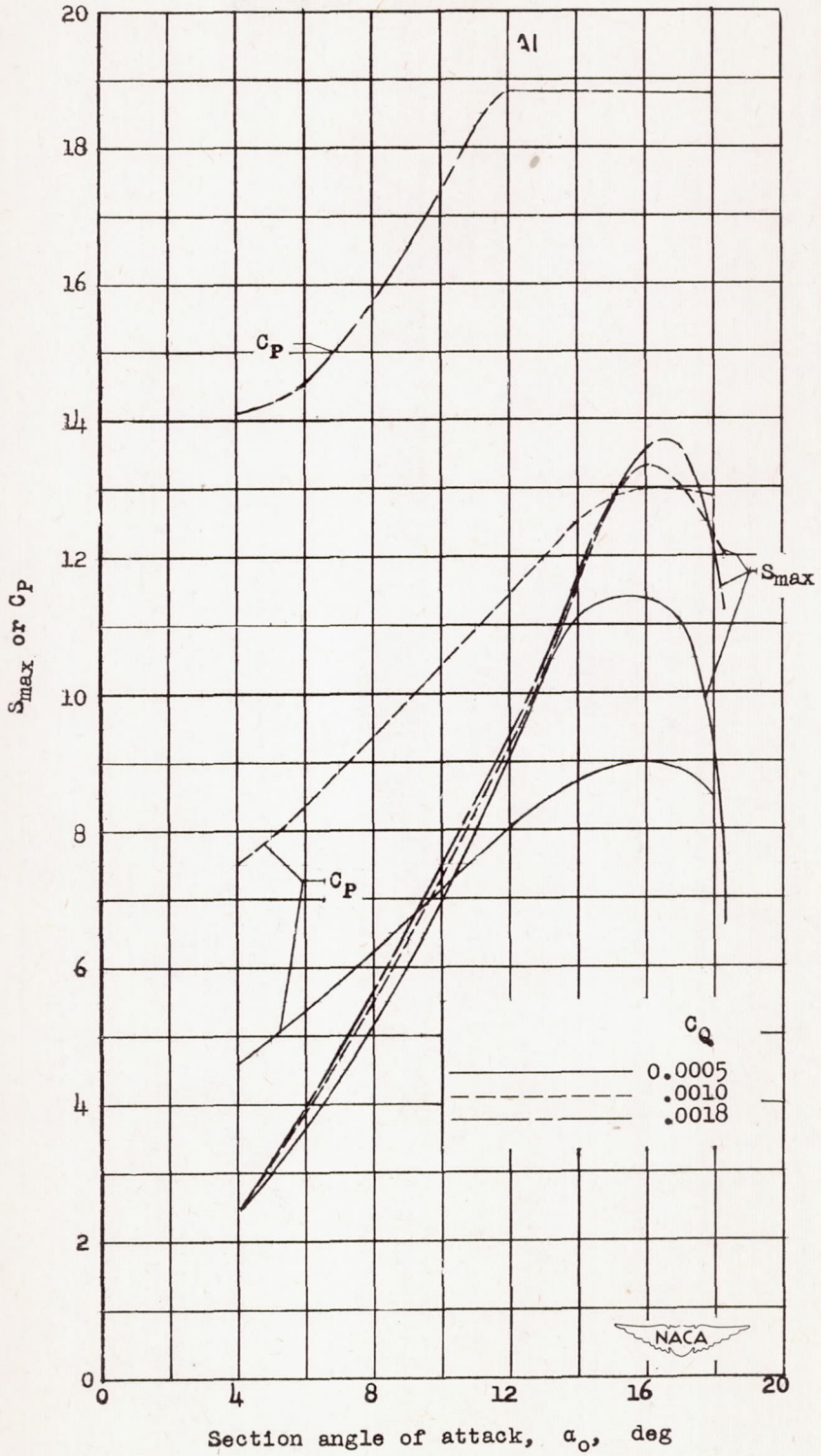

Figure 6.- Variation of S_{max} and C_P with section angle of attack for the NACA 64_1A212 airfoil with permeable nose. Configuration E; $R \approx 1.5 \times 10^6$.